JNeurosci
THE JOURNAL OF NEUROSCIENCE

Research Articles: Cellular/Molecular

Survival of a novel subset of midbrain dopaminergic neurons projecting to the lateral septum is dependent on NeuroD proteins

Shabana Khan[1], Simon Stott[1,+], Audrey Chabrat[2,3], Anna M. Truckenbrodt[1,*], Bradley Spencer-Dene[4], Klaus-Armin Nave[5], François Guillemot[1], Martin Levesque[2,3] and Siew-Lan Ang[1]

[1]*The Francis Crick Institute, Mill Hill Laboratory, The Ridgeway, Mill Hill, NW7 1AA, UK.*

[2]*Department of psychiatry and neurosciences, Université Laval, Québec, QC, G1V 0A6, Canada.*

[3]*Centre de recherche de l'Institut universitaire en santé mentale de Québec, chemin de la Canardière, Québec, G1J 2G3, Canada.*

[4]*The Francis Crick Institute, Lincoln's Inn Fields Laboratory, 44 Lincoln's Inn Fields Laboratory, London WC2A 3LY, UK.*

[5]*Department of Neurogenetics, Max Planck Institute of Experimental Medicine, Hermann-Rein-Str. 3, 37075 Göttingen, Germany.*

DOI: 10.1523/JNEUROSCI.2414-16.2016

Received: 29 July 2016

Revised: 7 November 2016

Accepted: 30 November 2016

Published: 27 January 2017

Author contributions: S.K., S.R.S., A.C., B.S.-D., M.L., and S.-L.A. designed research; S.K., S.R.S., A.C., A.T., and B.S.-D. performed research; S.K., S.R.S., A.C., A.T., K.-A.N., F.P.G., M.L., and S.-L.A. analyzed data; S.K., F.P.G., and S.-L.A. wrote the paper; K.-A.N. contributed unpublished reagents/analytic tools.

Conflict of Interest: The authors declare no competing financial interest.

This work was supported by funds from the Francis Crick Institute, which receives its core funding from UK Medical Research Council (MRC) and the Wellcome Trust. We thank Mary Green and Alessandro Pristera for thoughtful discussions and input.

Corresponding author: Siew-Lan Ang (same address as above), email: siew-lan.ang@crick.ac.uk

Cite as: J. Neurosci ; 10.1523/JNEUROSCI.2414-16.2016

Survival of a novel subset of midbrain dopaminergic neurons projecting to the lateral septum is dependent on NeuroD proteins

Shabana Khan[1], Simon Stott[1+], Audrey Chabrat[2,3], Anna M. Truckenbrodt[1*], Bradley Spencer-Dene[4], Klaus-Armin Nave[5], François Guillemot[1], Martin Levesque[2,3] and Siew-Lan Ang[1]

[1]The Francis Crick Institute, Mill Hill Laboratory, The Ridgeway, Mill Hill, NW7 1AA, UK.

[2]Department of psychiatry and neurosciences, Université Laval, Québec, QC, G1V 0A6, Canada.

[3]Centre de recherche de l'Institut universitaire en santé mentale de Québec, chemin de la Canardière, Québec, G1J 2G3, Canada.

[4]The Francis Crick Institute, Lincoln's Inn Fields Laboratory, 44 Lincoln's Inn Fields Laboratory, London WC2A 3LY, UK.

[5]Department of Neurogenetics, Max Planck Institute of Experimental Medicine, Hermann-Rein-Str. 3, 37075 Göttingen, Germany.

[*]Present Address: Institute of Developmental Genetics, Helmholtz Center Munich, German Research Center for Environmental Health, D-85764 Neuherberg, Germany

[+]Present address: John van Geest Centre for Brain Repair, University of Cambridge, Forvie Site, Robinson Way, Cambridge CB2 0PY, UK

Key words: dopaminergic neurons, ventral tegmental area, lateral septum, *Neurod6*, *Neurod1*. Abbreviated title: *Neurod6* defines a novel population of VTA neurons

Number of pages (29), 8 Figs. and 1 table, Number of words: Abstract (156), Introduction (557), Discussion (963).

The authors declare no competing financial interest.

Corresponding author: Siew-Lan Ang (same address as above), email: siew-lan.ang@crick.ac.uk

Acknowledgements

This work was supported by funds from the Francis Crick Institute, which receives its core funding from UK Medical Research Council (MRC) and the Wellcome Trust.

We thank Mary Green and Alessandro Pristera for thoughtful discussions and input.

ABSTRACT

Midbrain dopaminergic neurons are highly heterogeneous. They differ in their connectivity and firing patterns, and therefore in their functional properties. The molecular underpinnings of this heterogeneity are largely unknown and there is a paucity of markers that distinguish these functional subsets. In this paper, we report the identification and characterisation of a novel subset of midbrain dopaminergic neurons located in the ventral tegmental area that expresses the basic helix-loop-helix transcription factor, Neurogenic Differentiation Factor-6 (NEUROD6). Retrograde fluorogold tracing experiments demonstrate that *Neurod6*+ mDA neurons project to two distinct septal regions, the dorsal lateral and intermediate region of the lateral septum. Loss-of-function studies in mice demonstrate that *Neurod6* and the closely related family member *Neurod1* are both specifically required for the survival of this lateral-septum projecting neuronal subset during development. Our findings underscore the complex organisation of midbrain dopaminergic neurons and provide an entry point for future studies of the functions of the *Neurod6*+ subset of midbrain dopaminergic neurons.

SIGNIFICANCE STATEMENT

Midbrain dopaminergic neurons regulate diverse brain functions, including voluntary movement and cognitive and emotive behaviours. These neurons are heterogeneous and distinct subsets are thought to regulate different behaviours. However, we currently lack the means to identify and modify gene function in specific subsets of midbrain dopaminergic neurons. In this study, we identify the transcription factor NEUROD6 as a specific marker for a novel subset of midbrain dopaminergic neurons in the ventral

midbrain that project to the lateral septum and we reveal essential roles for *Neurod1* and *Neurod6* in the survival of these neurons during development. Our findings highlight the molecular and anatomical heterogeneity of midbrain dopaminergic neurons and contribute to a better understanding of this functionally complex group of neurons.

INTRODUCTION

Midbrain dopaminergic (mDA) neurons are mostly found in the substantia nigra pars compacta (SNc) and ventral tegmental area (VTA) and regulate multiple brain functions, including voluntary movement, working memory, emotion and cognition (Bjorklund and Dunnett, 2007). These neurons project to the forebrain and were initially thought of as a homogenous group of neurons based on their common use of dopamine as a neurotransmitter for intercellular communication. However, it is now becoming clear that mDA neurons are heterogenous in regard to their target and afferent projections (Roeper, 2013; Beier et al., 2015; Menegas et al., 2015), firing patterns (Roeper, 2013) and gene expression profiles (Poulin et al., 2014), all of which impact on their functional properties. mDA neurons projecting to striatal spiny projection neurons in the nucleus accumbens medial shell use glutamate as a co-transmitter (Hnasko et al., 2010; Stuber et al., 2010), whereas those projecting to the dorsal striatum use GABA (Tritsch et al., 2012). Furthermore, intact-brain analyses using a combination of whole brain imaging, optogenetics, viral tracing and fiber photometry, has revealed that different subsets of SNc neurons contribute to different nigrostriatal circuits carrying different information streams (Lerner et al., 2015).

Despite the emerging evidence for functionally distinct subsets of mDA neurons, we still know little of the molecular underpinnings of this functional diversity. Recent transcriptome analyses of VTA and SNc mDA neurons have provided lists of genes differentially expressed between these two anatomically separable groups of neurons (Grimm et al., 2004; Chung et al., 2005). One of these differentially expressed genes is the basic helix-loop-helix transcription factor NEUROD6, alternatively known as NEX1, MATH2 and ATOH2. NEUROD6 belongs to the NEUROD subfamily of basic-helix-loop (bHLH) transcription factors, which consists of 4 members including NEUROD1, NEUROD2, NEUROD4 and NEUROD6 (Bertrand et al., 2002). NEUROD2 and NEUROD6 are both required for the fasciculation and directional growth of callosal axons in the mouse neocortex (Bormuth et al., 2013). NEUROD6 also specifies the fate of a subtype of retinal amacrine cells (Cherry et al., 2011; Kay et al., 2011) and it has been implicated in the survival of cultured rat pheochromocytoma PC12 cells, where it enhances mitochondrial biogenesis and regulates cytoskeletal organization (Uittenbogaard and Chiaramello, 2005; Uittenbogaard et al., 2010; Baxter et al., 2012). These important roles of NEUROD6 in neuronal differentiation and survival raised the possibility of similar roles for this factor in mDA neurons.

We have therefore investigated the role of NEUROD6 in the development of mDA neurons using gene expression analysis and retrograde fluorogold tracing experiments in wild-type and *Neurod6* null mutant mice (Goebbels et al., 2006). Our findings revealed that *Neurod6* is specifically expressed in a subset of mDA neurons in the VTA that project to the intermediate (LSi) and dorsal regions (LSd) of the lateral septum. *Neurod6* alone is required for the survival of LSi-projecting mDA neurons,

however some *Neurod6*+ neurons still develop normally in *Neurod6* mutant mice and send axons to the LSd. Given this partial loss of *Neurod6*+ mDA neurons, we also analysed *Neurod6 and Neurod1* double mutant embryos and found that *Neurod1* also regulates the survival of the *Neurod6*+ mDA neurons. This study has identified a novel subset of mDA neurons that projects to the lateral septum and has a unique molecular signature. Our results also demonstrate essential roles for *Neurod1* and *Neurod6* in this subset of mDA neurons during development.

MATERIALS AND METHODS

Generation and genotyping of mutant embryos and animals

Neurod6-Cre is a knock-in mouse line that expresses Cre recombinase under the control of *Neurod6 regulatory sequences* (Goebbels *et al*., 2006). We first generated $Neurod6^{Cre/+}$;$R26R^{YFP/YFP}$ mice (refered to henceforth as *Neurod6* control mice) by sequential breedings of $Neurod6^{Cre/+}$ animals (Goebbels *et al*., 2006) with $R26R^{YFP/YFP}$ reporter mice. We intercrossed control $Neurod6^{Cre/+}$;$R26R^{YFP/YFP}$ mice to generate $Neurod6^{Cre/Cre}$;$R26R^{YFP/YFP}$ single homozygous mutant embryos and mice. For double mutant studies, $Neurod1^{LacZ/+}$;$Neurod6^{Cre/+}$;$R26R^{YFP/YFP}$ mice were generated by breeding $Neurod1^{LacZ/+}$ mice (Miyata *et al*., 1999) with $Neurod6^{Cre/Cre}$;$R26R^{YFP/YFP}$ animals. These animals were then intercrossed to generate double homozygous mutant embryos and mice carrying different numbers of *Neurod1* and *Neurod6* mutant alleles. *Neurod6* and *Neurod1* heterozygous and homozygous allelic deletions were determined by PCR as described in Schwab et al., 2000 and Chao et al., 2007 respectively. All male and female animals used were from mixed background. At all times, animals were handled

according to the Society of Neuroscience policy on the use of animals in Neuroscience research, as well as the European Communities Council Directive.

Tissue Preparation

For *in situ* hybridisation and immunohistochemistry experiments, 2 months old adult animals were deeply anesthetised with ketamine-xylazine (10mg/mL and 1mg/ml, respectively) and were transcardially perfused with PBS (pH 7.4) followed by 4% (wt/vol) formaldehyde in phosphate buffered saline (PBS), pH 7.4. Embryonic, postnatal and adult brains were removed, immersion-fixed in fixative 4% (wt/vol) formaldehyde in 100mM phosphate buffer, pH 7.4 overnight at 4°C and subsequently cryoprotected in 30% (wt/vol) sucrose-PBS. Tissue samples were embedded in optimum cutting temperature (OCT) compound (VWR International, Poole, UK), and sectioned on a cryostat (CM3050S; Leica, Nussloch, Germany) as 20 µm sections on Superfrost Plus microscope slides (25 x 75 x 1,0 mm; Thermo Scientific) for embryonic brains and 35 – 50 µm free-floating sections for postnatal and adult brains.

For RNAscope experiments, adult animals were deeply anesthetised with ketamine-xylazine (10mg/mL and 1mg/ml, respectively) and were transcardially perfused with 10% neutral buffered formalin (NBF; Sigma-Aldrich). Brains were then removed and immersion-fixed in 10% NBF overnight at room temperature and then transferred into 70% ethanol for storage. Brains were subsequently embedded in paraffin wax and processed into 4 µm sections collected onto Superfrost Plus microscope slides (25 x 75 x 1,0 mm; Thermo Scientific) using the Leica RM2255 microtome.

In Situ Hybridisation

Section *in situ* hybridisations were performed as previously described (Vernay et al., 2005) or using the RNAscope® 2.0 HD Brown Chromogenic Reagent Kit according to the manufacturer's instructions (Advanced Cell Diagnostics, Hayward, CA). The following mouse antisense RNA probes have been used: *Neurod6* (Brohl et al., 2008), *Neurod1* (Lee et al., 1995), *TH* (Grima et al., 1985). For RNAscope experiments, target probes for *Neurod6* and *Grp* were designed by Advanced Cell Diagnostics. For each probe, a minimum of three control and three mutant brains were analysed at embryonic and adult stages.

Immunohistochemistry

For immunohistochemistry, sections were incubated overnight at 4°C with the appropriate primary antibody diluted in 1% (wt/vol) bovine serum albumin (BSA) in PBS with 0.1% Triton X-100. Sections were washed thoroughly and subsequently incubated for 1 hour at room temperature with a secondary antibody conjugated with a fluorochrome (Molecular Probes) diluted in 1% BSA in 100mM PBS. For nuclear staining, sections were incubated with 4',6- Diamidino-2-Phenylindole, Dihydrochloride (DAPI). Sections were then washed extensively overnight in 100mM PBS and mounted in Vectashield H-1000 (Vector Laboratories,Burlingame, CA).

The following primary antibodies were used: sheep anti-GFP (1:1000; Bio-RAD/ AbD Serotec), rabbit anti-TH (1:1000; Pelfreez), mouse anti-TH (1:500; Immunostar), sheep anti-TH (1:1000; Millipore); rabbit anti-OTX2 (1:500; Baas *et al*., 2000), goat anti-OTX2 (1:500; R&D Systems), mouse anti-CALBINDIN1 (1:1000; Swant), rabbit anti-ALDH1A1 (1:200; Abcam), mouse anti-NEUROD1 (1:500; Abcam), rabbit anti-

NEUROD2 (1:1000; Abcam) and rabbit anti-TOM20 (1:1000; Santa Cruz Biotechnology). The following secondary antibodies were used: Alexa Fluor 594 donkey anti-rabbit (1:300; Molecular Probes), Alexa Fluor 488 donkey anti-sheep (1:200; Molecular Probes), FITC donkey anti-sheep (1:200; Jackson ImmunoResearch Laboratories, Inc.), Alexa Fluor 647 donkey anti-mouse (1:200; Molecular Probes), Cy5 donkey anti-mouse (1:200; Jackson ImmunoResearch Laboratories, Inc.), Cy5 donkey anti-sheep (1:200; Jackson ImmunoResearch Laboratories, Inc.).

Cell Counting & Imaging

For each brain, 50uM free-floating coronal cryosections were collected from the caudal to the rostral midbrain for immunohistochemistry with TH and GFP primary antibodies. Free-floating sections were subsequently mounted onto slides from caudal to the rostral midbrain and imaged using the Olympus virtual Slide microscope VS120-L100-W, ZEISS Apotome.2 microscope and Leica TCS SP5 confocal microscope. YFP+/TH+ double-positive cells were counted for one hemisphere of all midbrain sections to determine both the (i) total cell number and (ii) spatial distribution in controls and mutants at E18.5, P3, P7, P14 and adult stage. For each stage, three control and three mutant brains were analysed. Image J (National Institutes of Health, NIH) software was used for cell quantification.

Statistical Analysis

Statistical analysis was performed only on cell counts of sections from the central mDA region. All sections through the central mDA region (bregma from -3.28 to -3.80 mm)

contained 3 VTA nuclei, the paranigral nucleus (PN) and parabrachial nucleus (PBP) and the posterior portion of the interfascicular nucleus (IF) (Oades and Halliday, 1987), SNc as well as two adjacent nuclei, the interpeduncular nucleus (IPN) and the reticular magnocellular nuclei (RMC) of the red nucleus (see schematic in Fig. 3I). Sections were matched according to the presence of these landmarks from the caudal to the rostral extent. Besides these anatomical features, the most rostral section of the central mDA region also has the emergence of the fasciculus retroflexus. For cell count comparisons between two groups, statistical significance was assessed using the unpaired Student's t tests to determine differences in both the distribution and total number of TH+/YFP+ cells of the VTA in *Neurod6* controls and *Neurod6* mutants. When comparing cell number differences between more than two groups (*Neurod6* control, *Neurod6* mutant and *Neurod1;Neurod6* double mutants), statistical significance was assessed by One-way ANOVA (GraphPad Prism) with Tukey's post-test and comparing the means of each group to the mean of every other group.

Assay for cell apoptosis

To detect cell apoptosis, terminal deoxynucleotidyl transferase-mediated biotinylated UTP nick-end labelling (TUNEL) assays were performed using the TACS® 2 TdT DAB *In Situ* Apoptosis Detection Kit (Trevigen, R&D Systems; 4810-30-K). TUNEL staining was performed according to manufacturer's instructions. Once TUNEL was completed, sections were then analysed for TH expression by immunohistochemistry.

Densitometry

For the quantification of fluorescent intensity, images were acquired in structured illumination mode to achieve optical sectioning. Signal intensity of mitochondrial TOM-20 levels in YFP+/TH+ and YFP-/TH+ cells were quantified by Fiji image processing package. Regions of interest (ROIs) were accurately drawn around individual TH+ (YFP+ and YFP-) cells and readings of fluorescence intensity were only measured from the TOM-20 channel. Only mDA neurons showing the nucleus in the optic sections were included in the analysis (over 200 neurons were analysed per cell type per genotype, from at least 5 pictures per group), and background fluorescence values were subtracted from all the readings.

Retrograde fluorogold axonal labeling

The retrograde tracer Fluorogold (Millipore) was injected into the lateral septum of *Neurod6*$^{Cre/+}$;*R26R*$^{YFP/YFP}$ and *Neurod6*$^{Cre/Cre}$;*R26R*$^{YFP/YFP}$ pups at postnatal day 10 (P10). Mice were anesthetized using isoflurane, and 1µl of Fluorogold (2% in 0.9% sodium chloride) and 2% biotin dextran amine, Molecular Probes) was injected in both hemispheres. We adapted the stereotaxic coordinates of the atlas of Developing Mouse Brain (Paxinos and Watson, 2007) and the glass microsyringe was placed in the brain with the tip at 0,3 mm anterior to Bregma, 0,2 mm lateral of the midline and 1,8 mm from the surface of the brain. Mice were sacrificed 3 days after injection for further analysis. Location of the injection sites were confirmed by staining the section with streptavidin-conjugated to Alexa Fluor 568 that binds to biotin dextran amine.

RESULTS

Neurod6 identifies a subset of OTX2+, ALDH1A1+, CALBINDIN1+ mDA neurons in the VTA

We first examined the expression of *Neurod6* in the mouse midbrain by RNA *in situ* hybridisation from embryonic days 12.5 (E12.5) onwards. *Neurod6* expression was not detected at E12.5 (data not shown) but transcripts were found localised in the ventral regions of the VTA at E15.5 (Fig. 1A,A') and E17.5 (1B,B'). To determine whether *Neurod6* is expressed in mDA neurons, immunohistochemistry for TH protein expression was conducted following detection of *Neurod6* transcripts. *Neurod6* transcripts were co-localised with TH protein in the VTA at embryonic stages (brown staining in Fig. 1A,A',B,B') and its expression was maintained in a subset of ventral VTA TH+ neurons in adult mice (Fig. 1C-D'). In contrast, *Neurod6* was not detected in TH+ neurons of the SNc at any stage (Fig. 1C-D' and data not shown). Altogether, these results demonstrate that *Neurod6* is specifically expressed in a small subset of mDA neurons in the VTA from E15.5. to adulthood.

To facilitate co-localization studies between *Neurod6* and other genes expressed in mDA neurons in the VTA, and since a NEUROD6-specific antibody is not available, we used a mouse line where the coding region of *Neurod6* has been replaced by the *Cre* recombinase gene (Goebbels et al., 2006). We permanently labelled the cells in which the *Neurod6* promoter has been active by breeding these $Neurod6^{Cre}$ mice to $R26R^{YFP}$ reporter mice that conditionally express YFP in a Cre-dependent manner. We first confirmed that the CRE recombinase protein is co-expressed with YFP in VTA TH+ mDA neurons of $Neurod6^{Cre/+};R26R^{YFP/YFP}$ mice at P3 (Fig. 2A) . We then showed that

YFP expression is similar to endogenous *Neurod6* expression in the VTA of heterozygous *Neurod6*$^{Cre/+}$;*R26R*$^{YFP/YFP}$ adult mice by conducting multiplex *in situ* hybridization using RNAscope® followed by GFP antibody labelling. Indeed, all YFP+ neurons expressed *Neurod6* in the adult VTA (Fig. 2B). Altogether, these results establish that YFP expression in *Neurod6*$^{Cre/+}$;*R26R*$^{YFP/YFP}$ mice faithfully reflects endogenous *Neurod6* expression, and that expression of *Neurod6* is maintained in neurons once it has been initiated. We therefore used YFP expression in these mice as a marker of *Neurod6*+ mDA neurons in subsequent experiments.

Earlier studies have shown that expression of the homeodomain-containing transcription factor OTX2 in the midbrain is restricted to mDA neurons in the VTA (Di Salvio et al., 2010b; Di Salvio et al., 2010a). Moreover, mDA neurons in the VTA can be further subdivided into dorsal, central and ventral layers based on co-expression of OTX2 with other markers including CALBINDIN1 and ALDH1A1 (Di Salvio et al., 2010a). We therefore performed triple antibody labelling experiments for TH, YFP and these three proteins individually, to compare their expression patterns with that of *Neurod6* in mDA neurons. Our results show that all *Neurod6*+ cells express OTX2 (Fig. 2D), CALBINDIN1 (Fig. 2E) and ALDH1A1 (Fig. 2F) indicating the existence of a group of VTA neurons co-expressing all four genes. We also compared the expression of YFP and another VTA-enriched gene, gastrin releasing peptide [GRP; Paul Allen Brain Atlas, (Chung et al., 2005)]. RNAscope experiments using a *Grp* probe followed by antibody staining for GFP in *Neurod6*$^{Cre/+}$;*R26R*$^{YFP/YFP}$ adult mice revealed that *Grp* was expressed in all *Neurod6*$^{+}$ mDA neurons as well as in some surrounding *YFP*$^{-}$ cells (Fig. 2C). In

summary, our expression studies have identified a novel subset of VTA mDA neurons that co-express *Neurod6*, OTX2, CALBINDIN1, ALDH1A1 and *Grp*.

Neurod6 is required for the survival of a subset of VTA mDA neurons

To determine the role of *Neurod6* in mDA neurons, we analysed *Neurod6*$^{Cre/Cre}$; *R26R*$^{YFP/YFP}$ homozygous mutant mice. The total number and spatial distribution of *Neurod6*+ mDA neurons along the rostral-caudal axis of the VTA were evaluated by immunohistochemistry for TH and YFP at E18.5, postnatal day 3 (P3), P14 and 2 months (Fig. 3A-H and data not shown). We focused our quantitative analysis on anatomically defined sections in the central mDA region (see Materials and Methods), which contain the highest numbers of Neurod6+ cells i.e. 48% of the total number of VTA Neurod6+ mDA neuron (1136 ± 82) (Fig. 3L-N) and displayed a loss of Neurod6+ mDA neurons. At E18.5, we did not observe a significant difference in the total numbers of YFP+/TH+ cell in the central mDA region between *Neurod6* mutant and control embryos (Table 1). At postnatal stages in contrast, there was a significant reduction in numbers of TH+/YFP+ mDA neurons in this region of *Neurod6* mutant compared to control mice (28% of control numbers at P3, 31% at P14 and 32% at 2 months; Fig. 3 and Table 1). The VTA in adult mice can be further subdivided into several nuclei, including the interfascicular nucleus (IF), dorsal (dPN) and ventral paranigral nucleus (vPN), and parabrachial nucleus (PBP) (Oades and Halliday, 1987). YFP+/TH+ cells were found in all these nuclei in wild-type mice (Fig. 3J) and were missing specifically in the IF, dPN and PBP in *Neurod6* mutant mice (Fig. 3K). Altogether, these results show that the deletion of *Neurod6* results in a loss of approximately 30% *Neurod6*+, TH+ mDA

neurons in the central mDA region between E18.5 and P3 that persists at adult stages. YFP+/TH+ mDA neurons that subsist in the absence of *Neurod6* are localised in the vPN and the PBP (Fig. 3K).

Next, we asked whether the absence of *Neurod6*+ neurons in *Neurod6* mutants from P3 onwards was due to apoptosis, and we defined the precise timing of elimination of these cells, by conducting TUNEL analysis between E18.5 and P3. Some cells in the VTA of *Neurod6* mutant mice at P2 were TUNEL+ and expressed TH, while TUNEL+ cells were very rarely observed in control mice at this stage (Fig. 4A), indicating that *Neurod6*+ VTA neurons die from apoptosis at early postnatal stages in the absence of *Neurod6*.

The mechanisms of *Neurod6*-mediated neuronal survival have been extensively studied in PC12 cells where *Neurod6* functions to protect against oxidative stress by sustaining mitochondrial mass (Uittenbogaard et al., 2010). To assess changes in mitochondrial mass prior to neuronal cell death in *Neurod6* mutant VTA neurons, we examined the expression of the mitochondrial import receptor subunit (TOM-20) at E18.5. TOM-20 expression level in YFP+/TH+ VTA neurons, measured by densitometric analysis, was significantly decreased in *Neurod6* mutant compared to control embryo (Fig. 4B). A smaller but significant reduction in TOM-20 labeling was also observed in YFP- (*Neurod6*-)/TH+ mDA neurons (Fig. 4B). These results indicate a robust reduction in mitochondrial mass in both *Neurod6*+ and *Neurod6*- mDA neurons, and the difference between these two neuronal populations is also significant. Therefore, the sustenance of a subset of VTA neurons by *Neurod6* is likely to involve the maintenance of their mitochondrial mass.

***Specific changes in axon projections of mDA neurons to the lateral septum in adult Neurod6* mutant mice**

The loss of a subset of VTA neurons in *Neurod6* mutant mice is likely to affect the connectivity between the VTA and other brain regions. To address this possibility, we first compared the axon projections of mDA neurons in adult *Neurod6* mutant and control mice by immunohistochemistry for TH. We analysed the neuronal projection targets of VTA neurons (A10) in the septum, prefrontal cortex, nucleus accumbens, amygdala and olfactory tubercle. In control mice, a dense arborisation of TH+ axons was observed in the intermediate lateral septum (LSi) and fine varicosities of TH+ mDA axons were found in the dorsal lateral septum (LSd) (Fig. 5A,B). The dense arbor in the LSi was completely absent in *Neurod6* mutants, while the axons of the LSd were unaffected (Fig. 5A,B). The specific loss of TH+ mDA axons in the LSi was also observed at P3, P7 and P14 (data not shown). We also examined the septal target site at E18.5 before the loss of YFP+ mDA neurons in mutant embryos, however TH+ fibres were not detected in the dorsal lateral septal areas of control embryos, suggesting that at this stage TH+ mDA axons have not yet reached this target site (Fig. 5C,D). Consequently, it was not possible to analyse axon targeting before cell death in *Neurod6* mutants. In contrast to the defects observed in the lateral septum, TH+ mDA axons in all other A10 neuronal target sites also appeared normal in *Neurod6* mutant mice (Fig. 5E-J). The loss of both *Neurod6*+ neurons and TH+ axonal projections in *Neurod6* mutant mice suggests that *Neurod6*+ VTA neurons project to the intermediate regions of the lateral septum.

Fluorogold retrograde labelling demonstrates that Neurod6+ mDA neurons project to the lateral septum

To determine whether the septum is a specific target site for *Neurod6*+ mDA neurons, we next performed fluorogold (FG) retrograde labelling experiments. FG was injected into the lateral septum of *Neurod6* control and mutant pups at P10 and retrograde transport of FG into cell bodies of mDA neurons was analysed at P13 (Fig. 6A). We first confirmed that FG had been specifically injected into the LSd and LSi regions of the septum by staining for biotin dextran amine (BDA), which was co-injected with the FG. Coronal sections of the forebrain at the level of the septum showed BDA+ fibres in the lateral septal region, but not in the adjacent striatal region (Fig. 6B). In the midbrain of *Neurod6*+ control mice at P13, FG labelled most YFP+/TH+ mDA neurons in the IF, dPN, vPN and PBP of the VTA, demonstrating that *Neurod6*+ mDA neurons are lateral septal-projecting neurons (Fig. 6C). In *Neurod6* mutant mice, intra-septal FG injections retrogradely labelled many of the YFP+/TH+ mDA neurons that remain in the vPN and PBP of the VTA, indicating that these neurons project to the LSd and their axons likely correspond to the remaining TH+ fibres in the LSd of *Neurod6* mutants (Fig. 6D). Altogether, these results suggest that the YFP+/TH+ mDA neurons missing in *Neurod6* mutant animals project to the LSi, while the remaining YFP+/TH+ cells in these mutants project to the LSd. In addition, some YFP-/TH+ mDA neurons are labelled by FG indicating that *Neurod6*- mDA neurons also project to the lateral septum (Fig. 6C,D).

Severe loss of Neurod6+ VTA neurons in Neurod1 and Neurod6 double mutants

Since *Neurod* family members share redundant roles in other parts of the nervous system, we next addressed the possibility that another *Neurod* gene promotes the survival of a subset of *Neurod6+* neurons in *Neurod6* mutants. We first examined the expression profiles of NEUROD1 and NEUROD2 in mDA neurons. *Neurod1* transcripts were detected by *in situ* hybridisation strongly in immature and weakly in mature mDA neurons at E13.5 and E14.5 (Fig. 7A,B). NEUROD1 expression analysed by immunohistochemistry of *Neurod6*$^{Cre/+;}$*Rosa26*$^{YFP/YFP}$ embryos was maintained in all mature TH+ mDA neurons including YFP+ (*Neurod6+)* mDA neurons at E18.5. In addition, *in situ* hybridization of *Neurod1* followed by immunohistochemistry of TH showed that this expression was maintained into the adult stage (Fig. 7D). In contrast, NEUROD2 analysed by immunohistochemistry, was not expressed in mDA neurons at E18.5 (Fig. 7D).

To determine whether *Neurod1* is required for the survival of *Neurod6*+ mDA neurons, we used mice carrying a null allele of *Neurod1* whereby *LacZ* replaces the *Neurod1* coding sequence (Naya et al., 1997; Miyata et al., 1999) to generate *Neurod1* and *Neurod6* (*Neurod1;Neurod6*) double mutant mice (*Neurod1*$^{LacZ/LacZ}$*;Neurod6*$^{Cre/Cre}$*;R26R*). The double homozygous mutants died shortly after birth at P0, as the *Neurod1*$^{LacZ/LacZ}$ single mutants that die from neonatal diabetes (Miyata et al., 1999). We therefore examined *Neurod6*+ VTA neurons at E18.5 and observed a severe loss of YFP+/TH+ mDA neurons in the VTA of *Neurod1;Neurod6* double homozygous mutants (Fig. 8F,G) compared to both control (Fig. 8A,G) and *Neurod6*$^{Cre/Cre}$ single mutant embryos (Fig. 8B,G), which do not show a cell loss at this

stage. Moreover, mice homozygous mutant for *Neurod1* and heterozygous for *Neurod6* (*Neurod1*$^{LacZ/LacZ}$;*Neurod6*$^{Cre/+}$) as well as mice homozygous mutant for *Neurod6* and heterozygous for *Neurod1* (*Neurod1*$^{LacZ/+}$;*Neurod6*$^{Cre/Cre}$) and double heterozygous mice (*Neurod1*$^{LacZ/+}$;*Neurod6*$^{Cre/+}$ mice) also present significant losses of YFP+/TH+ mDA neurons compared to *Neurod6*$^{Cre/Cre}$ single mutants at E18.5 (Fig. 8D-F respectively and Fig. 8G). These results suggest that both *Neurod1* and *Neurod6* contribute to the survival of VTA *Neurod6*+ neurons before birth, since loss of one copy of each gene reduces neuronal viability. They also suggest that *Neurod1* has a more important role than *Neurod6* in *Neurod6*+ neuron survival, since loss of one copy of *Neurod1* and one copy of *Neurod6* results in the loss of some neurons while loss of two copies of *Neurod6* has no effect at E18.5. However, the early postnatal death of double mutant mice precluded the analysis of mDA neurons and axonal projections at later stages. Earlier analysis of double mutant embryos was also not feasible since YFP, which serves to mark *Neurod6*+ mDA neurons, only becomes detectable at E18.5 (data not shown).

DISCUSSION

In this paper, we have identified a novel subset of mDA neurons in the VTA that are marked by expression of the bHLH transcription factor NEUROD6. *Neurod6*+ neurons express a combination of molecular markers including OTX2, ALDH1A1, CALBINDIN1 and *Grp* and project to the LSi and LSd regions of the forebrain. Genetic studies revealed that *Neurod6* alone is required for the survival of LSi-projecting *Neurod6*+ mDA neurons postnatally, while the survival of *Neurod6*+ mDA neurons are dependent on both *Neurod1* and *Neurod6* embryonically. These results have identified a

novel subset of mDA neurons projecting to the lateral septum and revealed essential roles for NEUROD-family proteins in regulating the survival of this mDA neuronal subset. Our molecular characterization of this population of neurons will also facilitate further genetic manipulations to study the functions of these septal-projecting mDA neurons.

NeuroD6 identifies a novel subset of VTA mDA neurons that project to the lateral septum

Despite increasing evidence of heterogeneity among mDA neurons, there is still a paucity of specific markers to identify distinct mDA neuron subsets. mDA neurons in the VTA have been subdivided into molecularly distinct subsets based on combinational expression of more broadly expressed genes (Di Salvio et al., 2010a). For example, OTX2, CALBINDIN1 and ALDH1A1 mark a ventral subset of VTA neurons, while OTX2+/CALBINDIN1+ and OTX+/GIRK2+ label central and medial VTA neurons, respectively. Our molecular characterisation shows that VTA mDA neurons can be further subdivided by the expression of *Neurod6*. Recent studies using single-cell transcriptome profiling have also identified a molecularly distinct subset of mDA neurons in the VTA that co-expresses *Otx2*, *Aldh1a1*, *Calb*, *Grp*, *Lpl* and *Adcyap1* (Poulin et al., 2014). Since *Neurod6*+ mDA neurons also express the first four of these markers, it is probable that *Neurod6* marks the same subset. *Neurod6* is however uniquely expressed in this neuronal subset, in contrast to OTX2, CALBINDIN1 and ALDH1A1, which all have a broader expression in mDA neurons (Di Salvio et al., 2010a; Poulin et al., 2014). Our anatomical studies also showed that *Neurod6*+ mDA neurons have a complex spatial organization and are distributed in the PB, PN and IF nuclei of the adult VTA.

444 We carried out fluorogold retrograde tracing experiments, which established that
445 *Neurod6*+ neurons project to the septum. In this region, *Neurod6*+ mDA neurons project
446 to both the LSi and LSd. Loss of TH+ fibres in the LSi of *Neurod6* mutants suggest that
447 LSi is uniquely targeted by *Neurod6*+ mDA neurons. In contrast, the remaining TH+
448 fibres in the LSd likely correspond to axon termini of both *Neurod6*+ and *Neurod6*-
449 mDA neurons since both populations were labelled by FG in the retrograde labelling
450 experiments. As VTA axonal projections are thought to be mainly unbranched (Yetnikoff
451 et al., 2014), we have not determined whether *Neurod6*+ mDA neurons also project to
452 other forebrain regions. However, recent studies using single-cell transfection with viral
453 vectors have suggested the existence of different subgroups of VTA neurons targeting
454 one or more forebrain structures (Aransay et al., 2015). *Neurod6* is also expressed in the
455 interpeduncular nucleus and TH- cells in the rostral linear nucleus of raphe (Fig. 3B, C);
456 hence it is difficult to specifically trace the axon projections of Neurod6+/TH+ mDA
457 neurons using stereotaxic viral injections. Instead, we plan to employ a dual recombinase
458 intersectional genetic strategy (reviewed in Dymecki and Kim, 2007) to determine the
459 full projection target(s) of *Neurod6*+/TH+ mDA neurons in future experiments.
460 Consistent with an earlier report in the rat, our results showed that TH+ axon
461 projections to the septum become established at early postnatal stages since the TH+
462 fibres were first observed in P3 pups and not in E18.5 embryos (Antonopoulos et al.,
463 1997). The role of dopamine in the lateral septum is poorly studied. Lesions of septal
464 dopaminergic terminals by injection of 6-hydroxydopamine into the lateral septum of rats
465 result in deficits in spatial memory tasks (Simon et al., 1986). Our molecular and
466 neuroanatomical characterization of *Neurod6*+ septal-projecting mDA neurons, including

their expression of the neuropeptide Grp that is implicated in the regulation of memory associated with fear and emotional arousal, social interaction and food intake (reviewed in (Roesler and Schwartsmann, 2012), will aid in classifying these neurons and studying their potential functions in regulating memory and emotional behaviours.

Neurod6 and _Neurod1_ regulate the survival of septal-projecting mDA neurons

Our analysis revealed a 30% reduction in the number of *Neurod6*+ mDA neurons in the VTA of *Neurod6* single mutant mice at P3, and this phenotype was maintained in adult mutant mice. Loss of these neurons was accompanied by loss of TH+ fibres in the LSi of *Neurod6* single mutants, indicating that *Neurod6* alone is required for the survival of LSi-projecting mDA neurons. Since NEUROD1 is also expressed in both immature and mature mDA neurons during development and since *Neurod6*+ mDA neurons are partially lost in *Neurod6* single mutants, we also analysed the phenotypes of *Neurod1;Neurod6* double mutant mice Severe loss of *Neurod6*+ mDA neurons occurred in double homozygous mice at E18.5, i.e. before the cells are lost in *Neurod6* single mutants. *Neurod6*+ mDA neurons were also lost in double heterozygous mice and in mice homozygous for the *Neurod1* mutation and heterozygous for the *Neurod6* mutation. Because of the unavailability of NEUROD6-specific antibodies, we cannot determine the status of *Neurod6*+ mDA neurons in *Neurod1* single mutants. Together, our genetic analysis demonstrates that both *Neurod6* and *Neurod1* contribute to the survival of *Neurod6*+ mDA neurons. It also suggests that *Neurod1* has a more important role than *Neurod6* for *Neurod6*+ mDA neuronal survival at E18.5 since loss of the two copies of *Neurod6* has no effect while loss of one copy of *Neurod1* and one copy of *Neurod6* reduces survival of these neurons before birth.

NEUROD6 has been shown to have a neuroprotective role in PC12 cells serum deprived or treated with the mitochondrial stressor rotenone, and to act by enhancing mitochondrial biogenesis (Uittenbogaard et al., 2010; Baxter et al., 2012). Consistent with these findings, we observed a decrease in mitochondrial mass before the death of *Neurod6* mutant mDA neurons, suggesting that defects in energy metabolism contribute to the apoptosis of these neurons. Support for this hypothesis comes from an earlier study indicating that NEUROD6 maintains the expression of nuclear-encoded mitochondrial factors know to regulate mitochondrial biogeneis in PC12 cells (Uittenbogaard and Chiaramello, 2005). Alternatively or in addition, changes in mitochondrial mass might be an indirect consequence of neurons undergoing apoptosis because *Neurod6* may also regulate the expression of trophic factors, such as brain-derived growth factor as has been shown for *Neurod2* (Olson et al., 2001). The latter mechanism could explain why surrounding *Neurod6*- mDA neurons also exhibit a decrease in mitochondrial mass. Further studies will be required to identify the mechanisms through which NEUROD family proteins regulate the survival of embryonic mDA neurons during development and to determine whether these proteins continue to have a survival role in these neurons during adult life.

REFERENCES

Antonopoulos J, Dinopoulos A, Dori I, Parnavelas JG (1997) Distribution and synaptology of dopaminergic fibers in the mature and developing lateral septum of the rat. Brain Res Dev Brain Res 102:135-141.

Aransay A, Rodriguez-Lopez C, Garcia-Amado M, Clasca F, Prensa L (2015) Long-range projection neurons of the mouse ventral tegmental area: a single-cell axon tracing analysis. Front Neuroanat 9:59.

Baxter KK, Uittenbogaard M, Chiaramello A (2012) The neurogenic basic helix-loop-helix transcription factor NeuroD6 enhances mitochondrial biogenesis and

518 bioenergetics to confer tolerance of neuronal PC12-NeuroD6 cells to the
519 mitochondrial stressor rotenone. Exp Cell Res 318:2200-2214.
520 Beier KT, Steinberg EE, DeLoach KE, Xie S, Miyamichi K, Schwarz L, Gao XJ, Kremer
521 EJ, Malenka RC, Luo L (2015) Circuit Architecture of VTA Dopamine Neurons
522 Revealed by Systematic Input-Output Mapping. Cell 162:622-634.
523 Bjorklund A, Dunnett SB (2007) Dopamine neuron systems in the brain: an update.
524 Trends in neurosciences 30:194-202.
525 Bormuth I, Yan K, Yonemasu T, Gummert M, Zhang M, Wichert S, Grishina O, Pieper
526 A, Zhang W, Goebbels S, Tarabykin V, Nave KA, Schwab MH (2013) Neuronal
527 basic helix-loop-helix proteins Neurod2/6 regulate cortical commissure
528 formation before midline interactions. The Journal of neuroscience : the
529 official journal of the Society for Neuroscience 33:641-651.
530 Brohl D, Strehle M, Wende H, Hori K, Bormuth I, Nave KA, Muller T, Birchmeier C
531 (2008) A transcriptional network coordinately determines transmitter and
532 peptidergic fate in the dorsal spinal cord. Dev Biol 322:381-393.
533 Cherry TJ, Wang S, Bormuth I, Schwab M, Olson J, Cepko CL (2011) NeuroD factors
534 regulate cell fate and neurite stratification in the developing retina. The
535 Journal of neuroscience : the official journal of the Society for Neuroscience
536 31:7365-7379.
537 Chung CY, Seo H, Sonntag KC, Brooks A, Lin L, Isacson O (2005) Cell type-specific
538 gene expression of midbrain dopaminergic neurons reveals molecules
539 involved in their vulnerability and protection. Hum Mol Genet 14:1709-1725.
540 Di Salvio M, Di Giovannantonio LG, Omodei D, Acampora D, Simeone A (2010a) Otx2
541 expression is restricted to dopaminergic neurons of the ventral tegmental
542 area in the adult brain. Int J Dev Biol 54:939-945.
543 Di Salvio M, Di Giovannantonio LG, Acampora D, Prosperi R, Omodei D, Prakash N,
544 Wurst W, Simeone A (2010b) Otx2 controls neuron subtype identity in
545 ventral tegmental area and antagonizes vulnerability to MPTP. Nat Neurosci
546 13:1481-1488.
547 Dymecki SM, Kim JC (2007) Molecular neuroanatomy's "Three Gs": a primer. Neuron
548 54:17-34.
549 Goebbels S, Bormuth I, Bode U, Hermanson O, Schwab MH, Nave KA (2006) Genetic
550 targeting of principal neurons in neocortex and hippocampus of NEX-Cre
551 mice. Genesis 44:611-621.
552 Grima B, Lamouroux A, Blanot F, Biguet NF, Mallet J (1985) Complete coding
553 sequence of rat tyrosine hydroxylase mRNA. Proceedings of the National
554 Academy of Sciences of the United States of America 82:617-621.
555 Hnasko TS, Chuhma N, Zhang H, Goh GY, Sulzer D, Palmiter RD, Rayport S, Edwards
556 RH (2010) Vesicular glutamate transport promotes dopamine storage and
557 glutamate corelease in vivo. Neuron 65:643-656.
558 Kay JN, Voinescu PE, Chu MW, Sanes JR (2011) Neurod6 expression defines new
559 retinal amacrine cell subtypes and regulates their fate. Nat Neurosci 14:965-
560 972.
561 Lee JE, Hollenberg SM, Snider L, Turner DL, Lipnick N, Weintraub H (1995)
562 Conversion of Xenopus ectoderm into neurons by NeuroD, a basic helix-loop-
563 helix protein. Science 268:836-844.

564 Lerner TN, Shilyansky C, Davidson TJ, Evans KE, Beier KT, Zalocusky KA, Crow AK,
565 Malenka RC, Luo L, Tomer R, Deisseroth K (2015) Intact-Brain Analyses
566 Reveal Distinct Information Carried by SNc Dopamine Subcircuits. Cell
567 162:635-647.
568 Menegas W, Bergan JF, Ogawa SK, Isogai Y, Umadevi Venkataraju K, Osten P, Uchida
569 N, Watabe-Uchida M (2015) Dopamine neurons projecting to the posterior
570 striatum form an anatomically distinct subclass. Elife 4:e10032.
571 Miyata T, Maeda T, Lee JE (1999) NeuroD is required for differentiation of the
572 granule cells in the cerebellum and hippocampus. Genes & development
573 13:1647-1652.
574 Naya FJ, Huang HP, Qiu Y, Mutoh H, DeMayo FJ, Leiter AB, Tsai MJ (1997) Diabetes,
575 defective pancreatic morphogenesis, and abnormal enteroendocrine
576 differentiation in BETA2/neuroD-deficient mice. Genes & development
577 11:2323-2334.
578 Oades RD, Halliday GM (1987) Ventral tegmental (A10) system: neurobiology. 1.
579 Anatomy and connectivity. Brain Res 434:117-165.
580 Olson JM, Asakura A, Snider L, Hawkes R, Strand A, Stoeck J, Hallahan A, Pritchard J,
581 Tapscott SJ (2001) NeuroD2 is necessary for development and survival of
582 central nervous system neurons. Dev Biol 234:174-187.
583 Poulin JF, Zou J, Drouin-Ouellet J, Kim KY, Cicchetti F, Awatramani RB (2014)
584 Defining midbrain dopaminergic neuron diversity by single-cell gene
585 expression profiling. Cell Rep 9:930-943.
586 Roeper J (2013) Dissecting the diversity of midbrain dopamine neurons. Trends
587 Neurosci 36:336-342.
588 Roesler R, Schwartsmann G (2012) Gastrin-releasing peptide receptors in the
589 central nervous system: role in brain function and as a drug target. Front
590 Endocrinol (Lausanne) 3:159.
591 Schwab MH, Bartholomae A, Heimrich B, Feldmeyer D, Druffel-Augustin S, Goebbels
592 S, Naya FJ, Zhao S, Frotscher M, Tsai MJ, Nave KA (2000) Neuronal basic
593 helix-loop-helix proteins (NEX and BETA2/Neuro D) regulate terminal
594 granule cell differentiation in the hippocampus. The Journal of neuroscience :
595 the official journal of the Society for Neuroscience 20:3714-3724.
596 Simon H, Taghzouti K, Le Moal M (1986) Deficits in spatial-memory tasks following
597 lesions of septal dopaminergic terminals in the rat. Behav Brain Res 19:7-16.
598 Stuber GD, Hnasko TS, Britt JP, Edwards RH, Bonci A (2010) Dopaminergic terminals
599 in the nucleus accumbens but not the dorsal striatum corelease glutamate.
600 The Journal of neuroscience : the official journal of the Society for
601 Neuroscience 30:8229-8233.
602 Tritsch NX, Ding JB, Sabatini BL (2012) Dopaminergic neurons inhibit striatal output
603 through non-canonical release of GABA. Nature 490:262-266.
604 Uittenbogaard M, Chiaramello A (2005) The basic helix-loop-helix transcription
605 factor Nex-1/Math-2 promotes neuronal survival of PC12 cells by modulating
606 the dynamic expression of anti-apoptotic and cell cycle regulators. Journal of
607 neurochemistry 92:585-596.
608 Uittenbogaard M, Baxter KK, Chiaramello A (2010) The neurogenic basic helix-loop-
609 helix transcription factor NeuroD6 confers tolerance to oxidative stress by

triggering an antioxidant response and sustaining the mitochondrial biomass. ASN Neuro 2:e00034.

Vernay B, Koch M, Vaccarino F, Briscoe J, Simeone A, Kageyama R, Ang SL (2005) Otx2 regulates subtype specification and neurogenesis in the midbrain. The Journal of neuroscience : the official journal of the Society for Neuroscience 25:4856-4867.

Yetnikoff L, Lavezzi HN, Reichard RA, Zahm DS (2014) An update on the connections of the ventral mesencephalic dopaminergic complex. Neuroscience 282:23-48.

Figure and Table Legends

Figure 1. Selective expression of *Neurod6* in mDA neurons in the VTA. ***A-D,*** *In situ* hybridization for *Neurod6* combined with immunohistochemistry for TH showing that *Neurod6* expression is restricted to TH+ mDA neurons located in ventral regions of the VTA from E15.5 to adult stage (***A-C***). In contrast**,** *Neurod6* is not expressed in TH+ mDA neurons in the SNc (**D**). ***A'-D',*** Higher magnification of boxed regions in corresponding panels A-D. Scale bars: 200 µm (A), 10 µm (A').

Figure 2. Identification of a novel subset of mDA neurons in the VTA that expresses *Neurod6*, OTX2, CALBINDIN1, RALDH1 and *Grp*. ***A,*** Double antibody labelling showing that CRE is co-expressed with YFP in TH+ mDA neurons in the VTA of *Neurod6*$^{Cre/+}$ pups at P3. ***B,*** *In situ* hybridization of *Neurod6* combined with immunohistochemistry for YFP showing that all YFP+ cells express *Neurod6* transcripts (red arrows) in adult *Neurod6*$^{Cre/+}$ mice. A few YFP- cells also express *Neurod6* transcripts (blue arrowheads). ***C***, *In situ* hybridization of *Grp* combined with immunohistochemistry for YFP showing that *Grp* transcripts are detected in both YFP+ (red arrows) and YFP- (blue arrowheads) cells in the VTA of adult

Neurod6$^{Cre/+}$ mice. ***D, E, F,*** Triple antibody labelling showing that all YFP+TH+ mDA neurons express OTX2 (***D***), CALBINDIN1 (***E***) and RALDH1 (***F***) in the VTA of adult *Neurod6*$^{Cre/+}$ mice. Dotted vertical lines indicate the midline of the section. Arrowheads indicate triple-labelled cells observed in the red and green channels only. Scale bars: 100 µm (A), 200 µm (B-C, higher magnifications in D-F), 20 µm (D-F).

Figure 3. Partial reduction in the number of *Neurod6+* mDA neurons in the absence of NEUROD6 function. ***A-H,*** Immunohistochemistry for both YFP and TH on coronal sections from the caudal to the rostral extent of the mDA region at P14. Reduced numbers of YFP+,TH+ neurons are observed in the central mDA region (B,C,F,G), while there is no apparent change in the numbers of YFP+TH+ mDA neurons in the rostral and caudal midbrain at P14. ***I***, Schematic diagram showing the positions of mDA nuclei in the VTA and anatomical landmarks. ***J,K***, Double antibody labelling of YFP and TH on a section through the central mDA region shows that YFP+TH+ neurons are lost mostly in the dorsal paranigral (PN), parabrachial (PBP) and interfascicular (IF) nuclei (only the YFP channel is shown). ***L-N***, Graph showing the number of YFP+,TH+ mDA neurons analysed by immunohistochemistry on coronal midbrain sections from the caudal to the rostral extent of the mDA region at different stages. *Neurdo6+* mDA neurons in the VTA are lost predominantly in the central mDA region corresponding to sections demarcated by red vertical lines. RMC; reticular magnocellular nuclei of the red nucleus; ml, medial lemiscus; SNc, substantia nigra pars compacta; VTA, ventral tegmental area. Error bars denote

SEM. * p<0.05; **p<0.01 (Student's t test). Dotted vertical lines indicate the midline of the section. Scale bars: 200 µm (A), 100 µm (J).

Figure 4. Loss of NEUROD6 function results in cell death and reduced mitochondrial mass in mDA neurons. ***A***, Apoptotic cells (arrowheads) revealed by TUNEL analysis are observed in the TH+ mDA region of *Neurod6* mutant, but not in control pups at P2. ***B***, A representative mDA neuron immunolabelled for TH, YFP and TOM-20 that was used in quantitative analysis of mitochondria mass is shown. Dotted lines demarcate cell boundary. **C,** Reduction in mitochondrial mass measured by the mean fluorescence (normalised to cell area) of neurons analysed by immunohistochemistry with TOM20, TH and YFP (AU, arbitrary units) in *Neurod6* control and mutant embryos at E18.5. n, number of neurons analysed. ** p<0.01; ****p<0.0001 (one-way ANOVA, with Tukey's post-test). Scale bars: 200 µm (A), 25 µm (B).

Figure 5. TH+ mDA axon projections to the intermediate region of the lateral septum are specifically missing in adult *Neurod6* mutant mice. ***A,B,*** TH immunohistochemistry show specific loss of axon projections (arrowheads) to the intermediate region (Lsi) but not to the dorsal region (LSd) of the lateral septum in *Neurod6* mutant adult mice. ***C,D,*** TH+ axon projections from mDA neurons have reached the reached the dorsal lateral septum (LS) at E18.5. ***E-J***, TH+ mDA neuronal projections to other target sites of the VTA including nucleus accumbens (NAc), olfactory tubercle (OT), amygdala (Amg) and prefrontal cortex (PFC) appear normal

684 in *Neurod6* mutant compared to control adult mice. TH+ axons of SNc mDA neuronal
685 projections to the striatum (Str) were also unaffected. MS, medial septum; LSv,
686 lateral septum, ventral; MS, medial septum; cc, corpus callosum; ac, anterior
687 commissure. Insets in ***G-J*** show higher magnification of boxed region. Scale bars:
688 200 µm (A).
689
690 **Figure 6**. Fluorogold retrograde labelling experiments show that *Neurod6+* mDA
691 neurons project to the dorsolateral and intermediate region of the lateral septum.
692 ***A*,** Schematic diagram indicating the position of fluorogold injection in the injected
693 brain and the schedule of the experiment. ***B*,** Biotin dextran amine is detected
694 specifically in the intermediate region (LSi) as well as the dorsal region (LSd) of the
695 lateral septum but not in the adjacent striatal regions. C, D. Injection of fluorogold
696 into the septal region results in its retrograde transport of fluorogold into YFP+ TH+
697 mDA cell bodies in *Neurod6* control and mutant mice by P13. Scale bars: 100 µm
698 (A,B), 200 µm (C), 20 µm (higher magnification).
699
700 **Figure 7.** *Neurod1* but not *Neurod2* is expressed in mDA neurons. ***A,B,*** *In situ*
701 hybridization show that *Neurod1* transcripts are expressed strongly and weakly
702 respectively in immature and mature (arrows) in mDA neurons located ventral to
703 the floor plate of the midbrain at E13.5 (A) and E14.5 (B). ***C-E*** This expression,
704 detected by triple immunolabeling with NEUROD1, TH and YFP antibodies, is
705 maintained in mature YFP+ and TH+ mDA neurons at E18.5 (C-C") and in adult (D)
706 *Neurod6* control mice by *in situ* hybridization of *Neurod1* followed by

immunohistochemistry of GFP and TH. ***E,*** In contrast, NEUROD2 was not detected in mDA neurons and in only sporadic TH- cells at E18.5 by immunohistochemistry in sections of rostral and central mDA regions. Insets in C', C" and D show higher magnification of corresponding boxed areas. White arrowheads in C' and yellow arrowhead in C" indicate double and triple-labelled cells respectively. Scale bars: 100 µm (A-C), 10 µm (C', C"), 100 µm (E).

Figure 8. *Neurod1* is also required for the survival of *Neurod6+* mDA neurons.

A-F, YFP+,TH+ mDA neurons are lost at E18.5 in *Neurod1;Neurod6* double mutants carrying different copy numbers of *Neurod1* and *Neurod6* mutant alleles. Immunohistochemistry of YFP and TH shows that reduced numbers of YFP+/TH+ mDA neurons are observed in coronal sections of the central midbrain in double mutant embryos carrying 2 (***C***), 3 (***D,E***) or 4 *Neurod1;Neurod6* mutant alleles (***F***). In contrast, *Neurod6* single homozygous mutants present no change in YFP+/TH+ expression in mDA neurons at E18.5 (***B***). ***G***, Bar graph showing percentage changes of the number of YFP+/TH+ mDA neurons in the central mDA region of *Neurod1;Neurod6* double and *Neurod6* single mutant embryos normalised to $Neurod6^{Cre/+}$ control embryos. Error bars denote SEM. N=3 per genotype. * $p<0.05$; **$p<0.01$; ***$p<0.0001$ (one-way ANOVA, with Tukey's post-test). Scale bars: 100 µm (A).

729 **Table 1.** This table shows the raw data of the numbers of mDA neurons counted per
730 brain hemisphere in the central mDA region and the results from statistical analysis,
731 comparing cell counts between *Neurod6* mutant and control brains at each stage
732 using the unpaired Student's t test.
733
734 **Table 2.** This table shows the raw data of the numbers of mDA neurons counted per
735 brain hemisphere in the central mDA region among *Neurod6* single,
736 *Neurod1;Neurod6* double mutant and control brains at E18.5.
737

Figure 1

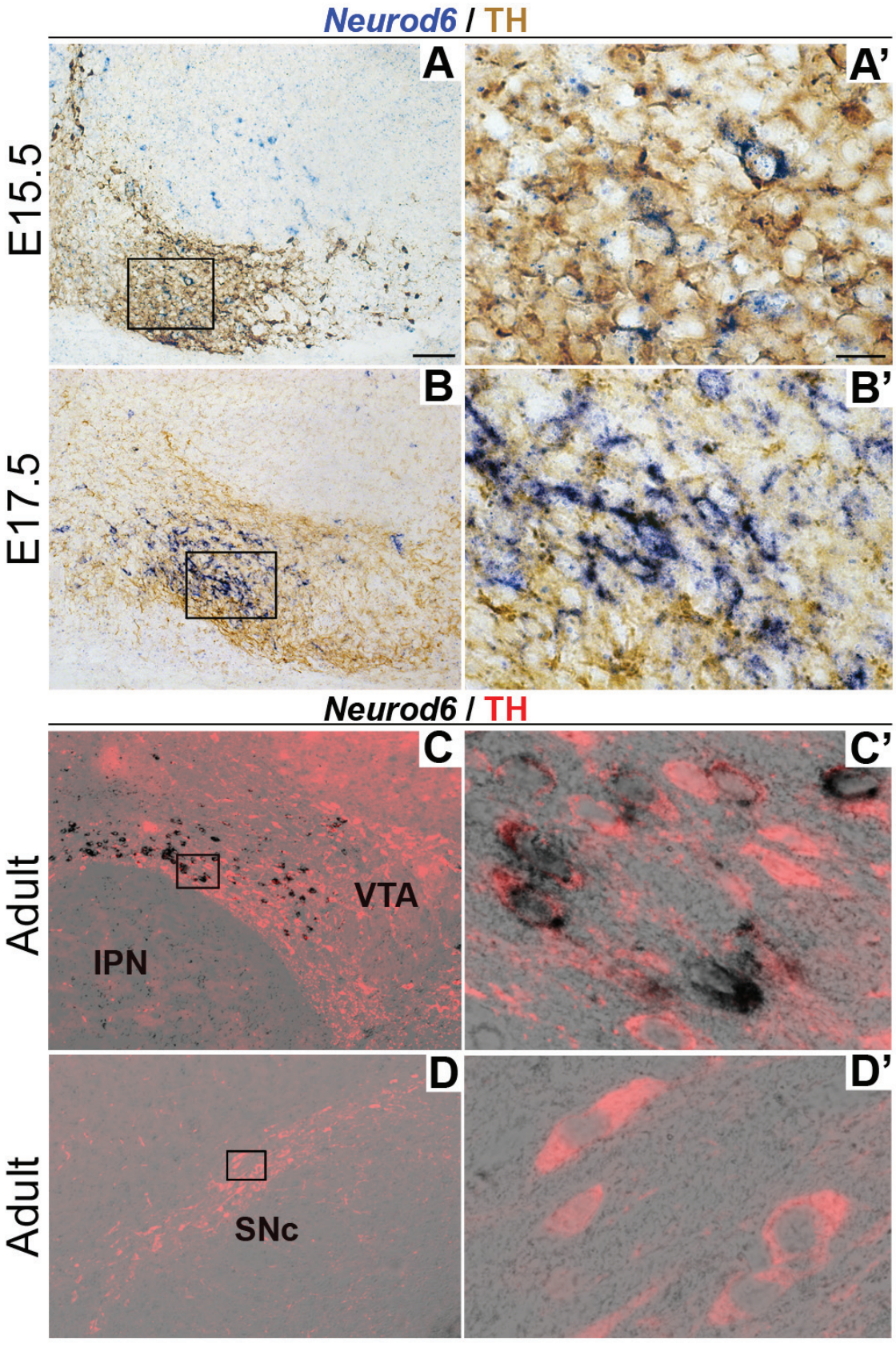

Figure 2

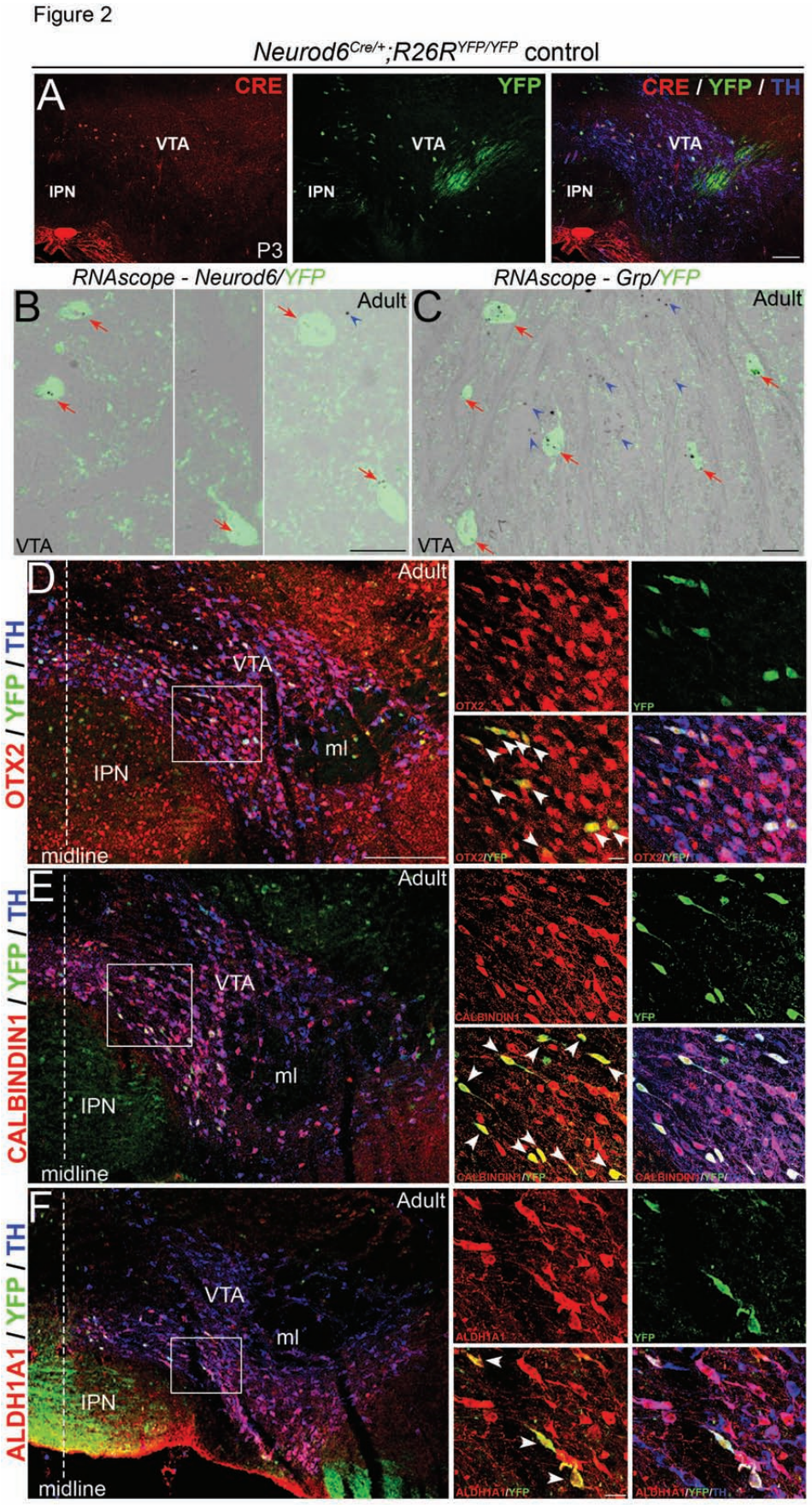

Figure 3

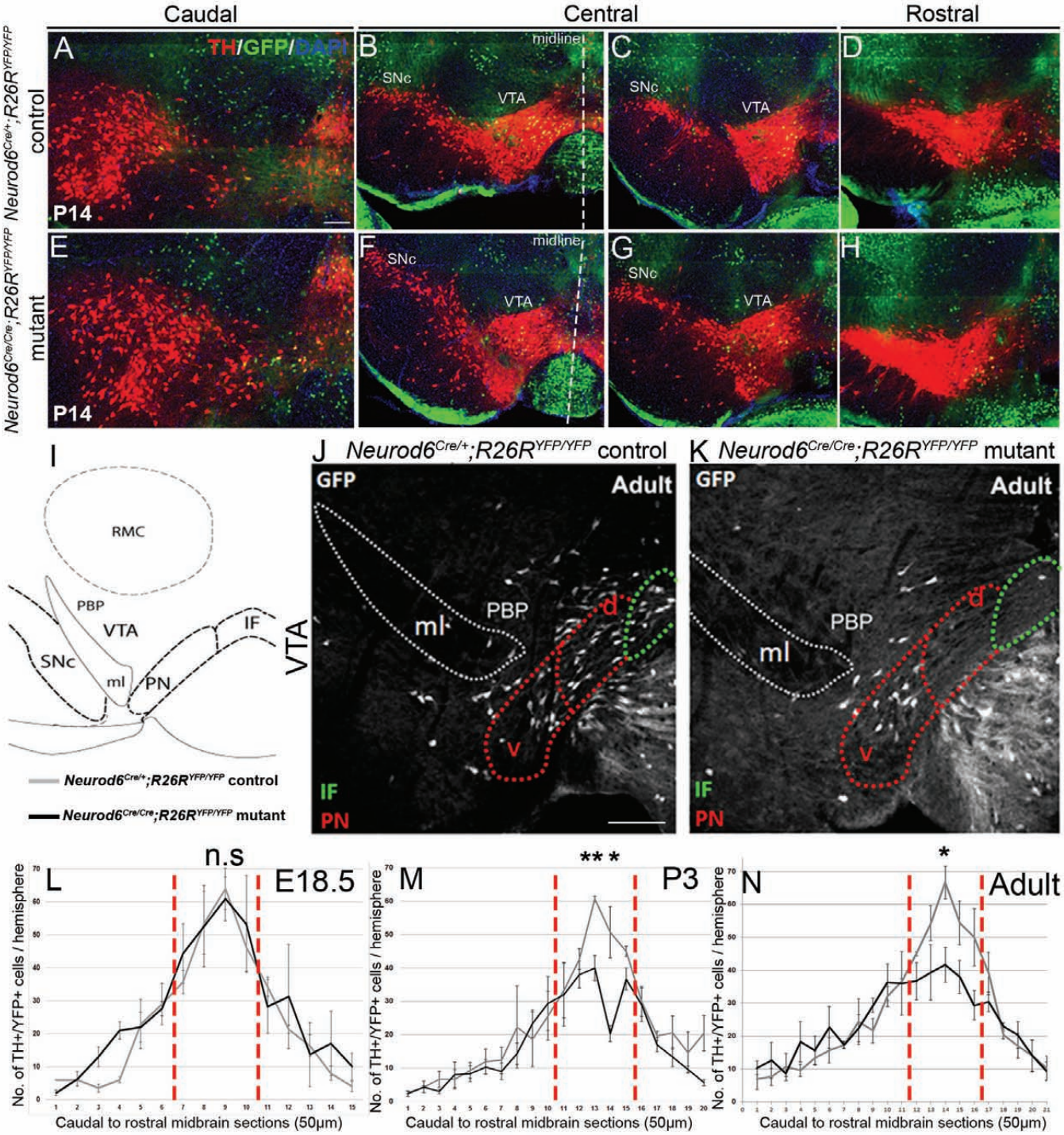

Figure 4

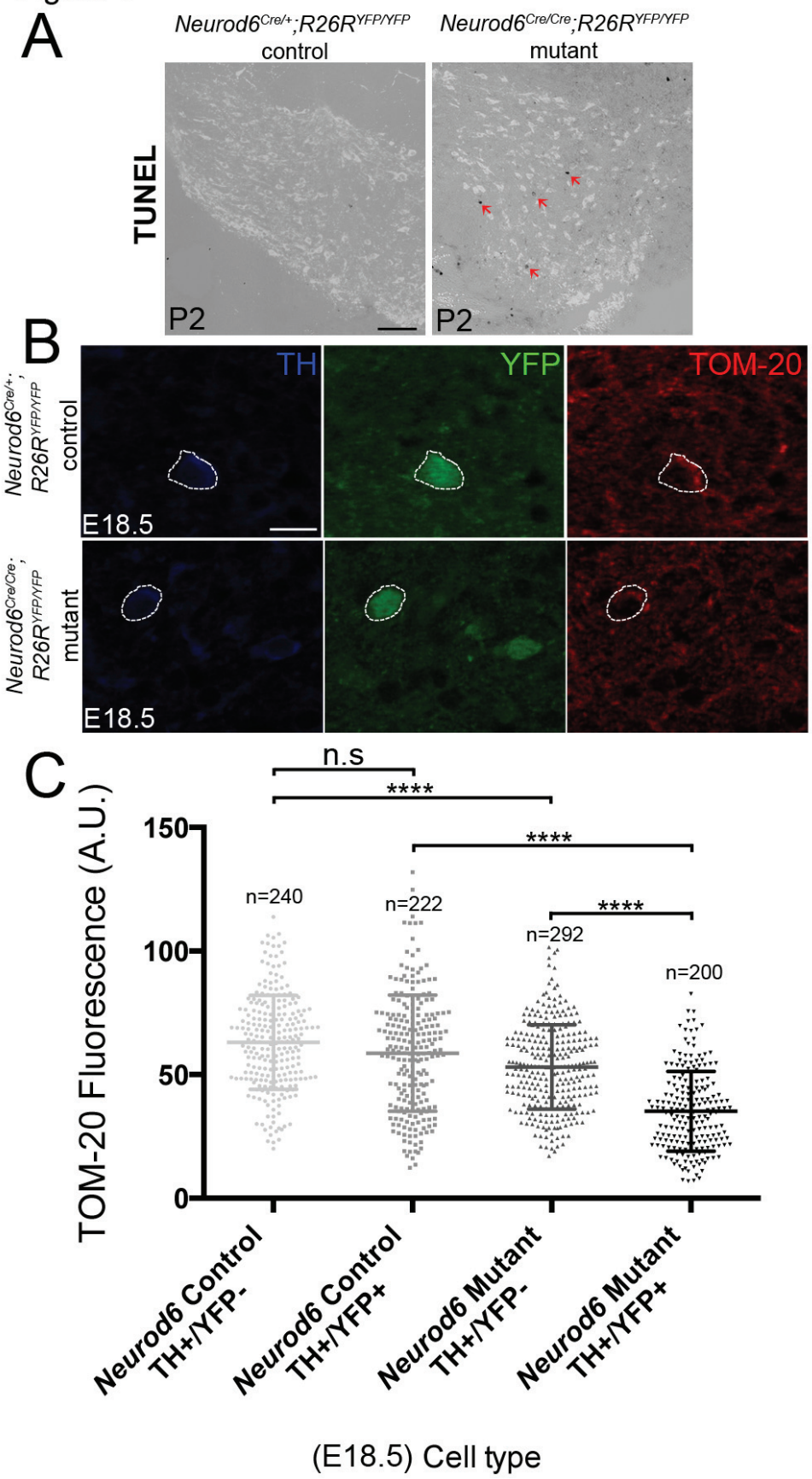

Figure 5

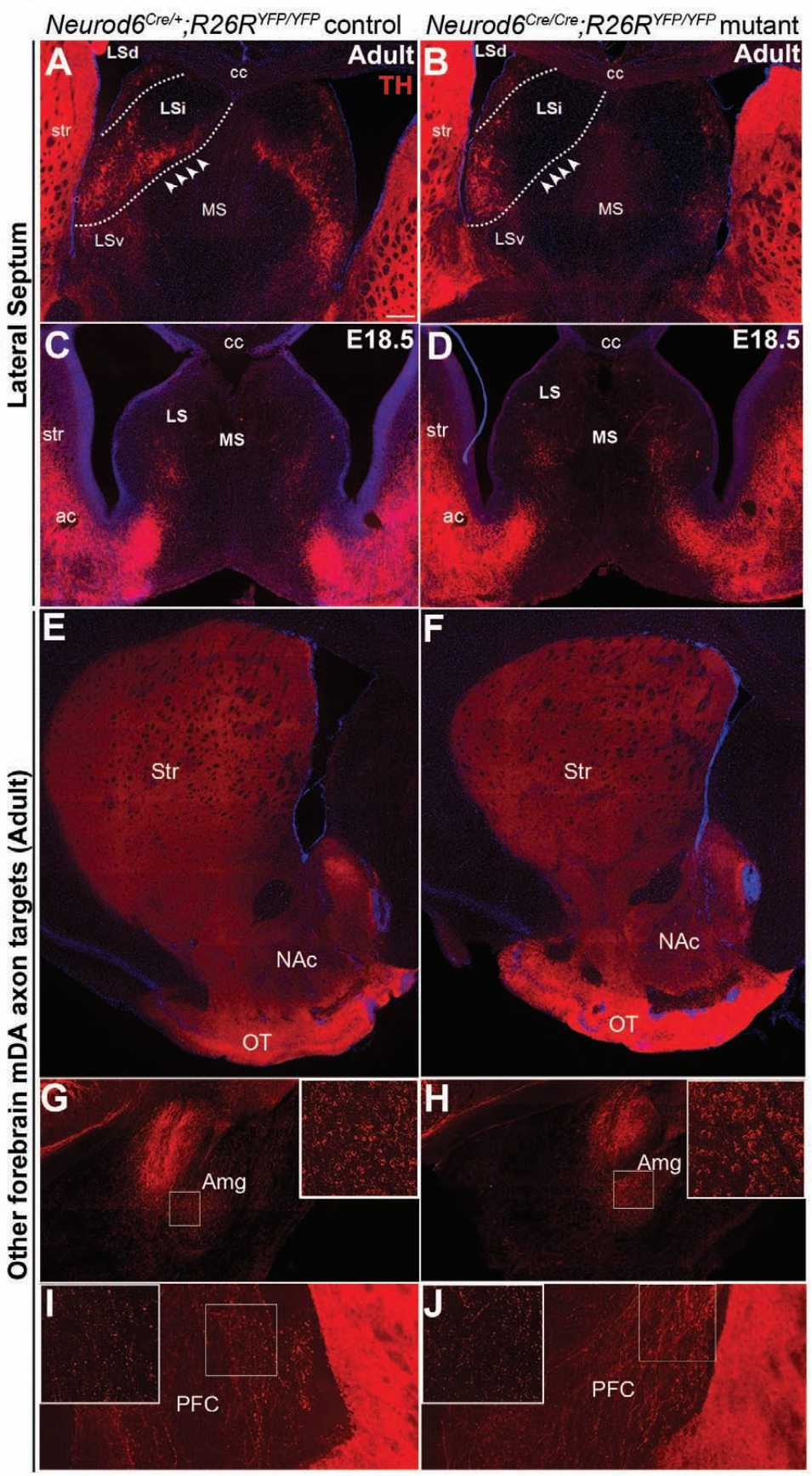

Figure 6

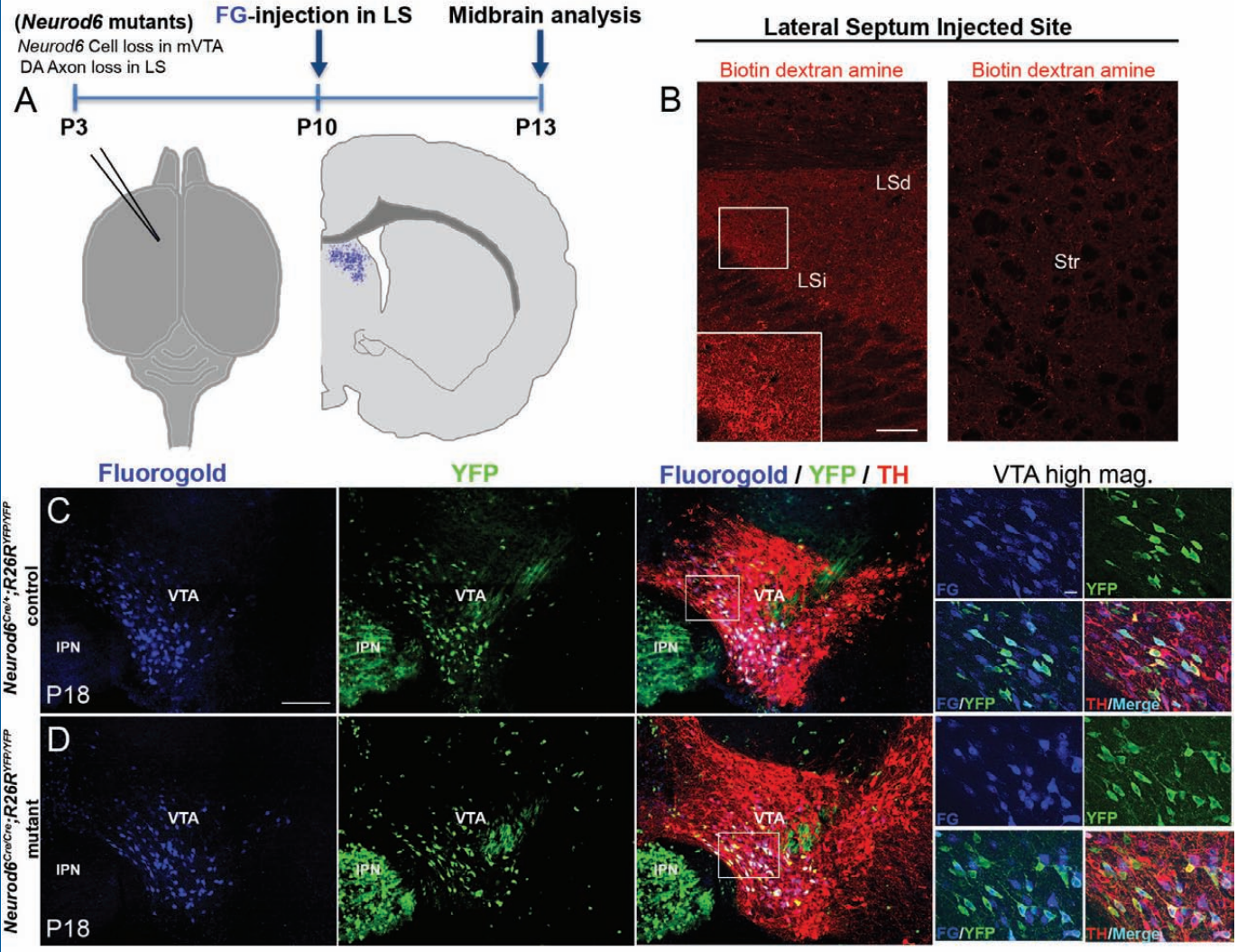

Figure 7

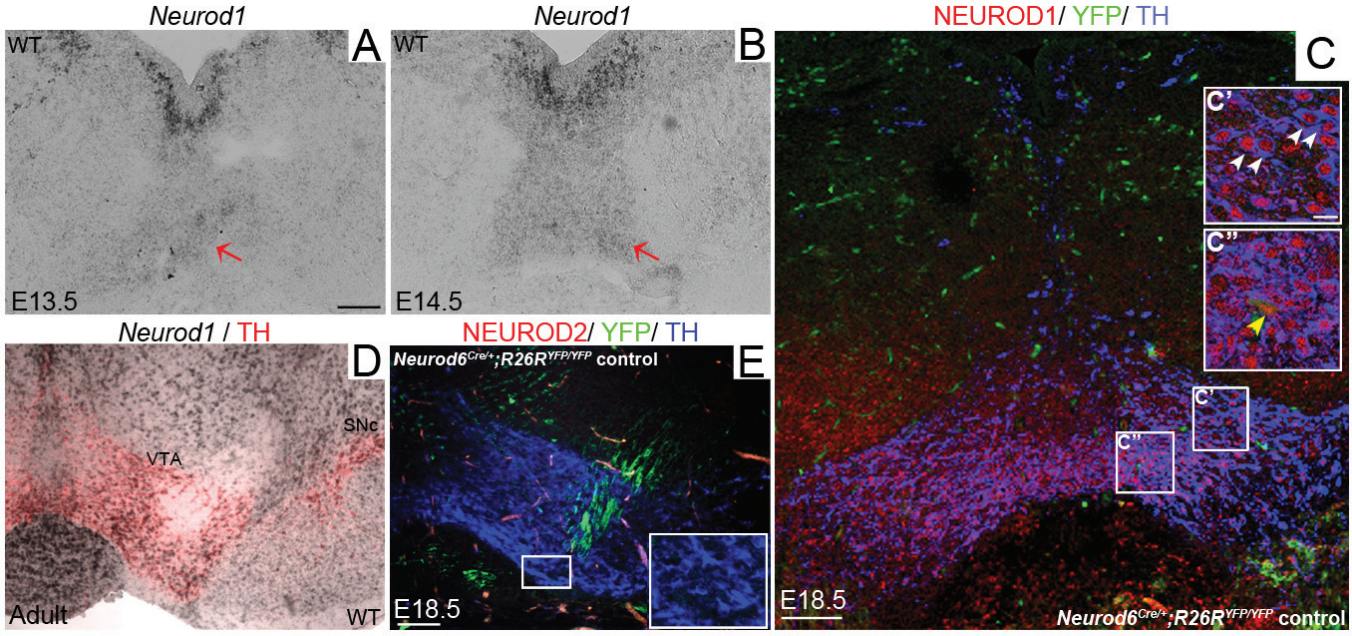

Figure 8

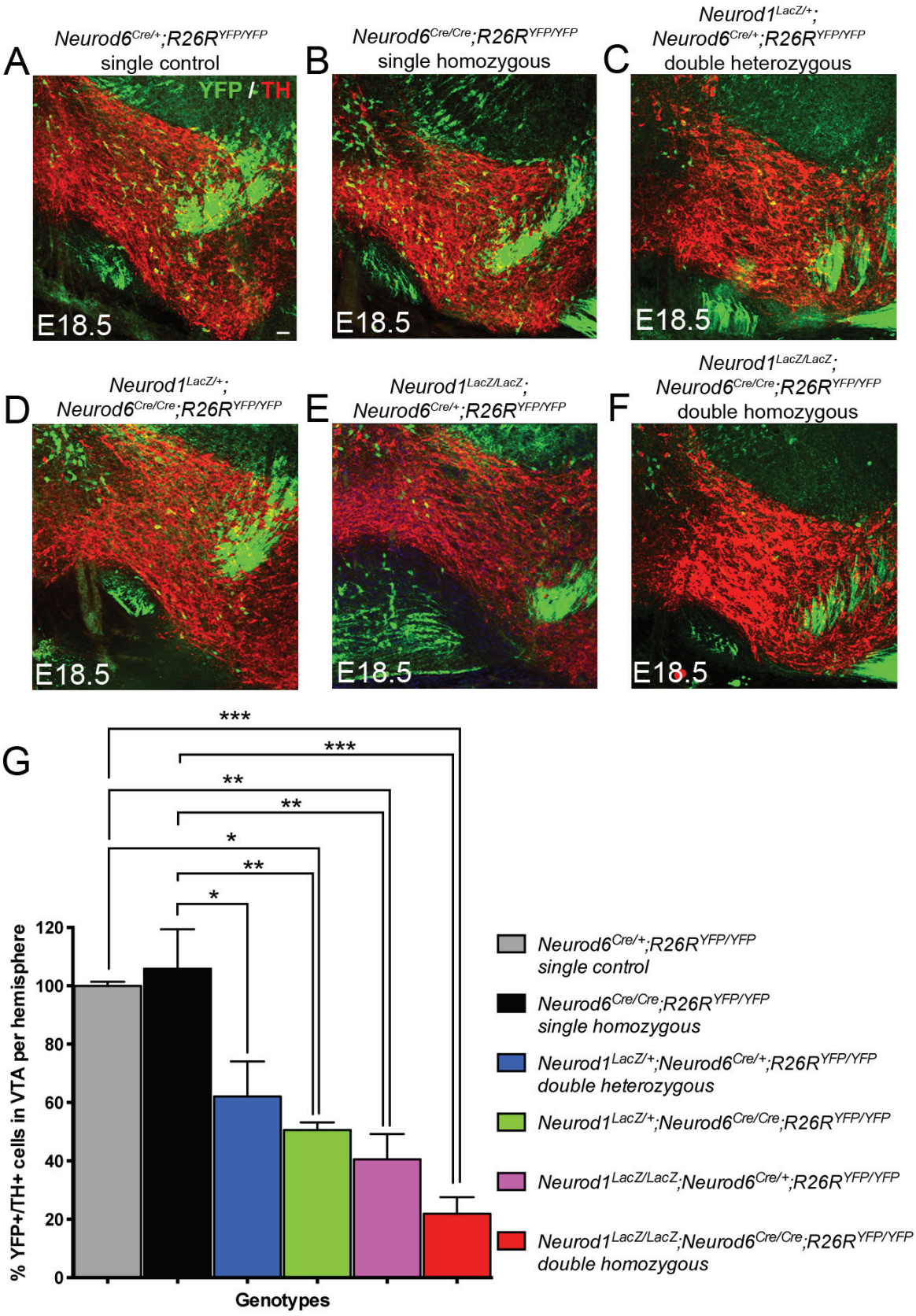

Table 1. Loss of YFP+/TH+ cells in the central mDA region of *Neurod6*$^{Cre/Cre}$;*R26R*$^{YFP/YFP}$ mutants per brain hemisphere

	E18.5	P3	P14	Adult
n	3	3	3	3
Neurod6 Controls (*Mean* ± *S.E.M*)	200 ± 3	232 ± 5	207 ± 1	270 ± 16
Neurod6 Mutants (*Mean* ± *S.E.M*)	211 ± 27	167 ± 10	143 ± 14	185 ± 26
% of YFP+/TH+ mDA cells lost in mutants relative to controls	N/A	28%	31%	32%
Average number of cells lost in mutants (*Mean* ± *S.E.M*)	N/A	65 ± 14	65 ± 14	85 ± 15
significance	n.s	**	**	*
p-value	0.69	0.004	0.001	0.05

n, number of brain samples analysed; S.E.M, standard error of the mean; n.s, not significant.

Table 2. Total numbers of YFP+/TH+ cells counted in the central mDA region of *Neurod6* and *Neurod1* double mutants per brain hemisphere at E18.5

Genotype	*n*	(Mean ± S.E.M)
Neurod6$^{Cre/+;}$*R26R*$^{YFP/YFP}$ single controls	3	200 ± 3
Neurod6$^{Cre/Cre}$;*R26R*$^{YFP/YFP}$ single homozygous	3	211 ± 27
Neurod1$^{LacZ/+}$;*Neurod6*$^{Cre/+;}$*R26R*$^{YFP/YFP}$ double heterozygous	3	124 ± 24
Neurod1$^{LacZ/+}$;*Neurod6*$^{Cre/Cre}$;*R26R*$^{YFP/YFP}$	3	101 ± 5
Neurod1$^{LacZ/LacZ}$;*Neurod6*$^{Cre/+}$;*R26R*$^{YFP/YFP}$	3	81 ± 17
Neurod1$^{LacZ/LacZ}$;*Neurod6*$^{Cre/Cre}$;*R26R*$^{YFP/YFP}$ double homozygous	3	44 ± 11

n, number of brain samples analysed; S.E.M, standard error of the mean